Thermal carrier emission and nonradiative recombinations in nonpolar (Al,Ga)N/GaN quantum wells grown on bulk GaN

P. Corfdir, A. Dussaigne, H. Teisseyre, T. Suski, I. Grzegory et al.

Citation: J. Appl. Phys. **111**, 033517 (2012); doi: 10.1063/1.3681816
View online: http://dx.doi.org/10.1063/1.3681816
View Table of Contents: http://jap.aip.org/resource/1/JAPIAU/v111/i3
Published by the American Institute of Physics.

Thermal carrier emission and nonradiative recombinations in nonpolar (Al,Ga)N/GaN quantum wells grown on bulk GaN

P. Corfdir,[1,a)] A. Dussaigne,[1] H. Teisseyre,[2,3] T. Suski,[3] I. Grzegory,[3] P. Lefebvre,[4] E. Giraud,[1] J.-D. Ganière,[1] N. Grandjean,[1] and B. Deveaud-Plédran[1]
[1]*Institute of Condensed Matter Physics, Ecole Polytechnique Fédérale de Lausanne (EPFL), CH-1015 Lausanne, Switzerland*
[2]*Institute of Physics, Polish Academy of Sciences, 02-668 Warsaw, Poland*
[3]*Institute of High Pressure Physics, Polish Academy of Sciences, 01-142 Warsaw, Poland*
[4]*Laboratoire Charles Coulomb – UMR5221 – CNRS – Université Montpellier 2, 34095 Montpellier, France*

(Received 17 October 2011; accepted 5 January 2012; published online 8 February 2012)

We investigate, via time-resolved photoluminescence, the temperature-dependence of charge carrier recombination mechanisms in nonpolar (Al,Ga)N/GaN single quantum wells (QWs) grown via molecular beam epitaxy on the *a*-facet of bulk GaN crystals. We study the influence of both QW width and barrier Al content on the dynamics of excitons in the 10-320 K range. We first show that the effective lifetime of QW excitons τ increases with temperature, which is evidence that nonradiative mechanisms do not play any significant role in the low-temperature range. The temperature range for increasing τ depends on the QW width and Al content in the (Al,Ga)N barriers. For higher temperatures, we observe a reduction in the QW emission lifetime combined with an increase in the decay time for excitons in the barriers, until both exciton populations get fully thermalized. Based on analysis of the ratio between barrier and QW emission intensities, we demonstrate that the main mechanism limiting the radiative efficiency in our set of samples is related to nonradiative recombination in the (Al,Ga)N barriers of charge carriers that have been thermally emitted from the QWs. © *2012 American Institute of Physics*. [doi:10.1063/1.3681816]

I. INTRODUCTION

Currently, there is growing interest in the study of nonpolar nitride-based heterostructures with the aim of realizing high-power optoelectronic devices operating in the UV range. When growth is along the polar *c*-axis, polarization discontinuities at the interfaces of III-nitride heterostructures induce huge built-in electric fields along the growth axis,[1] and it is thus mandatory to grow thin quantum wells (QWs) in order to keep an optimal overlap between electron and hole wave functions.[2] Conversely, the growth of wide QWs is of key importance when designing high-power nitride-based optoelectronic devices: they indeed allow a reduction of the carrier density in the QW, thereby lessening the efficiency of Auger-like mechanisms.[3] The absence of polarization discontinuity at the interfaces of *a*- or *m*-plane heterostructures makes possible the growth of thick QWs without any decrease of the radiative efficiency of the device.[4] However, the growth of nonpolar GaN on foreign substrates results in structures in which exciton dynamics is limited by capture on extended defects.[5,6] A further step toward the improvement of the light emission efficiency has been taken recently in the use of a nonpolar *a*-facet of bulk GaN substrates for the growth of an (Al,Ga)N/GaN QW.[7] In that work, we indeed show that the use of a nonpolar GaN substrate allows for the fabrication of QWs in which the exciton lifetime is limited by radiative processes for temperatures below (typically) 150 K. Although room-temperature cathodoluminescence experiments demonstrated that dislocations did not play any significant role in the dynamics of excitons, a drop in the exciton photoluminescence (PL) effective decay time was observed from 150 to 300 K.

In the present study, we therefore investigate the mechanisms responsible for the temperature dependence of exciton recombination dynamics in *a*-plane (Al,Ga)N/GaN QWs grown on low-dislocation density bulk GaN substrates. We investigate the influence of both the QW width and the barrier Al content. For all samples, we measure purely radiative recombination mechanisms from 10 to ~150 K. At higher temperatures, we observe a drop in the QW PL effective decay time, accompanied by an increase in the (Al,Ga)N barrier PL decay time. Supported by a theoretical model that accounts for the equilibrium between charge carriers in the QW and in the (Al,Ga)N barriers, we deduce from our experiments that the mechanism limiting the radiative efficiency of the present GaN QWs at 300 K is nonradiative recombination in the disordered (Al,Ga)N barriers of excitons and free electron-hole pairs that have thermally escaped the QWs.

II. EXPERIMENTAL DETAILS

a-plane GaN substrates have been prepared by means of a combination of the high-pressure solution method and hydride vapor phase epitaxy (HVPE) (details of the growth of nonpolar GaN substrates are given in Ref. 8). We then deposited, via ammonia molecular beam epitaxy, a 200 nm thick GaN epilayer on top of the substrates. Five different samples were grown, including one single 2 nm thick GaN

[a)]Author to whom correspondence should be addressed. Electronic mail: pmc53@cam.ac.uk. Present address: Cavendish Laboratory, J. J. Thomson Avenue, Cambridge CB3 0HE, United Kingdom.

TABLE I. QW width L_{QW} and $Al_xGa_{1-x}N$ barrier Al content x of the investigated samples. The emission properties of the different samples at 10 K are also given: E_{10K}, δ, E_{loc}, and τ_{loc} stand, respectively, for the QW emission energy, the QW emission full width at half maximum, the exciton localization energy, and the localized QW exciton PL lifetime.

Samples			QW emission properties at 10 K			
No.	x(%)	L_{QW}(nm)	E_{10K}(eV)	δ(meV)	E_{loc}(meV)	τ_{loc}(ps)
N1	12	2	3.585	15	16 ± 2	160
N2	6	2	3.540	13	14 ± 1	150
N3	6	4	3.494	10	4 ± 1	130
N4	6	7	3.483	8	2 ± 1	100

QW sandwiched between $Al_{0.12}Ga_{0.88}N$ barriers (sample N1) and three single GaN QW samples with a barrier Al content set to 6% and QW widths of 2, 4, and 7 nm (samples N2, N3, and N4, respectively; see Table I). In all cases, the bottom and top (Al,Ga)N barrier thicknesses were set to 160 and 30 nm, respectively. In addition to the QW samples, we grew, under the same conditions, an *a*-plane 190 nm thick $Al_{0.06}Ga_{0.94}N$ layer (sample N5). Note that for sample N5, an additional 1.5 nm thick AlN spacer was inserted between the GaN and the $Al_{0.06}Ga_{0.94}N$ epilayers. Non-resonant PL experiments were carried out with the third harmonic ($\lambda = 280$ nm) of a mode-locked Al_2O_3:Ti laser (average power, pulse width, and repetition rate of 50 μW, 2 ps, and 80.7 MHz, respectively). The laser beam was focused down to a 40 μm diameter spot on the surface of the sample. Assuming homogeneous excitation across the laser spot and accounting for the reflections of the laser beam on the window of the cryostat and on the surface of the sample, we estimated the total photogenerated carrier density as $N_{tot} = 5 \times 10^{10}$ cm^{-2} per pulse. The time-resolved PL was analyzed with a 1200 grooves/mm grating followed by a streak camera synchronized with the laser. Finally, envelope function calculations including the variational modeling of excitonic effects were performed using a finite difference method in which the in-plane and on-axis relative motions of electrons and holes are assumed to be independent.[9]

III. RESULTS AND DISCUSSION

A. Low-temperature emission properties

Figure 1 shows time-integrated PL spectra for the three $Al_{0.06}Ga_{0.94}N$/GaN QW samples investigated here (samples N2, N3, and N4). At 10 K, the QW emission of sample N2 is centered at 3.54 eV and presents a full width at half maximum $\delta = 13$ meV. When the QW width is increased from 2 to 7 nm, the emission energy of the fundamental QW exciton decreases to 3.483 eV, which agrees well with the trend expected for polarization free QWs.[10,11] In parallel, the thicker the QW, the narrower its emission (Table I), a finding that we relate to the combination of reduced penetration of exciton wave function into the disordered alloy barriers and a smaller effect of well width variations on quantized energies. In particular, the $\delta = 8$ meV emission linewidth we measure for the 7 nm thick QW (sample N4) attests to the

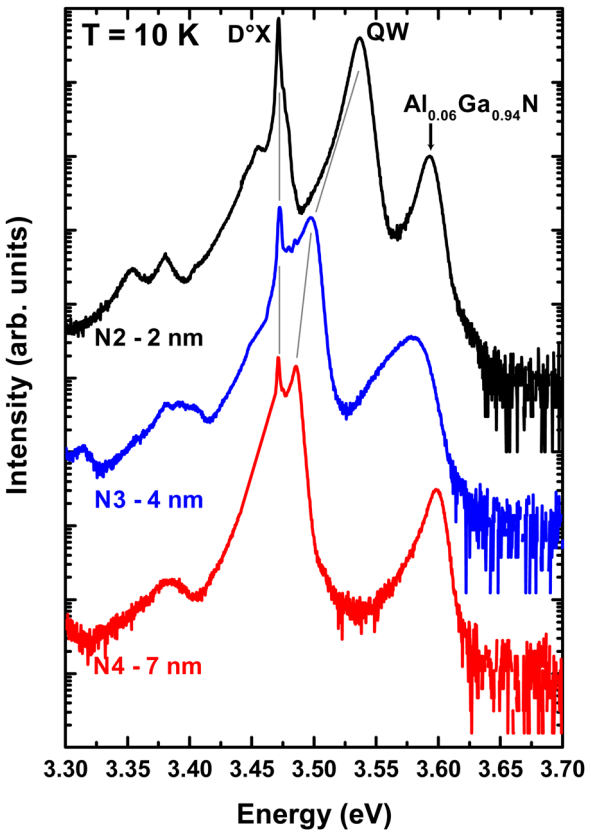

FIG. 1. (Color online) Time-integrated spectra at 10 K for 2, 4, and 7 nm thick $Al_{0.06}Ga_{0.94}N$/GaN QWs (from top to bottom). Spectra have been shifted vertically for clarity. Gray lines are guides for the eye.

improved material quality achieved when growing nonpolar (Al,Ga)N/GaN QWs on bulk GaN, relatvie to what is obtained for MBE-grown *a*-plane QW samples deposited on epitaxial lateral overgrown (ELO) GaN ($\delta = 18$ meV in the case of a 7 nm $Al_{0.05}Ga_{0.95}N$/GaN QW).[11] We also underline the fact that the 8 meV linewidth measured for sample N4 is only 2 meV larger than what has been reported for state-of-the-art *c*-plane $Al_{0.05}Ga_{0.95}N$/GaN QWs grown via metal-organic vapor phase epitaxy.[12] In addition to the emission from the fundamental QW exciton, we observe for all samples a strong emission centered at 3.471 eV that arises from excitons bound to donors in the GaN substrate (D°X).[13] We note the absence of the band at 3.42 eV that is usually observed with nonpolar GaN layers deposited on lattice mismatched substrates and ascribed to exciton recombination on basal plane stacking faults (BSFs).[14,15] Given that even when their local density is as low as 10^4 cm^{-1}, BSFs exhibit intense PL,[16] the present observation is evidence that, if present, stacking faults in our samples are only in low density and do not affect excitons confined in the QWs. Coming to the emission from the $Al_{0.06}Ga_{0.94}N$ barriers, we observe that its peak energy at 10 K ranges between 3.58 and 3.60 eV. Similar to a previous work on nonpolar (Al,Ga)N/GaN deposited on sapphire,[11] we attribute these fluctuations in the (Al,Ga)N emission energy to fluctuations in the Al composition originating from adatom incorporation anisotropy when growing on nonpolar planes.

At 10 K, QW excitons are localized at potential fluctuations induced by a single monolayer variation of the QW

width.[17,18] When T increases, exciton delocalization into the whole two-dimensional quasi-continuum of states is activated, resulting in a blueshift of the QW emission (Fig. 2). We can therefore access the exciton localization energies from the T-dependence of QW PL energies, and we observe that for a constant barrier Al content of 6% (samples N2, N3, and N4), the exciton localization energy increases from 2 to 14 meV when the well width decreases from 7 to 2 nm (Table I). Coming to the QW decay times at 10 K, we observe that they are quite short compared to those reported in Refs. 4, 6, 11, 19, and 20 (Fig. 3). Although the short lifetimes observed here might misleadingly suggest that the PL of the present QWs is governed by nonradiative processes, they on the contrary are evidence of better control of the QW interface roughness in heterostructures grown on bulk GaN crystals, as discussed in Ref. 7. We also observe that at 10 K, for quantum wells grown on bulk GaN crystals with similar barrier Al contents, the thinner the QW, the smaller the localized exciton decay rate (Fig. 3). This is not surprising because a narrower QW means deeper localization. Consequently, the narrower the QW, the larger the extent of the QW localized exciton wave function in reciprocal space,[21,22] and the longer the radiative lifetime, as observed experimentally in Ref. 23.

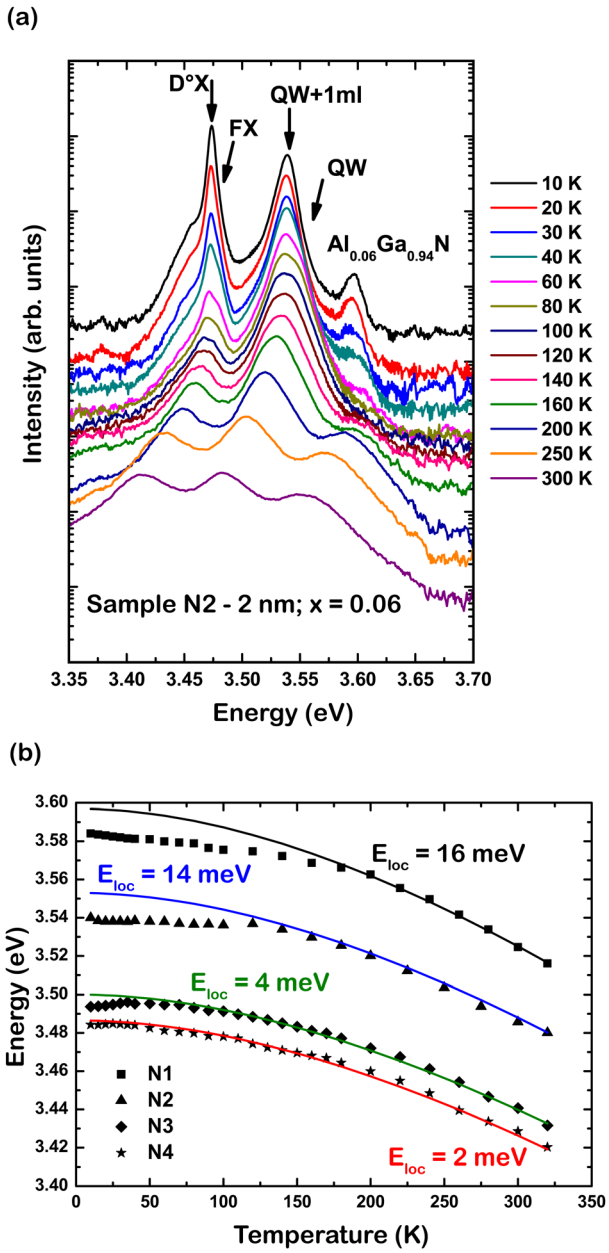

FIG. 2. (Color online) (a) Time-integrated spectra for 2 nm thick $Al_{0.06}Ga_{0.94}N$/GaN QWs (sample N2) between 10 and 320 K. Spectra have been shifted vertically for clarity. For $T > 200$ K, the high-energy slopes of these semi-logarithmic plots of PL spectra for the QWs and for the barrier are the same, indicating that the exciton populations of wells and barriers are thermalized. "QW" and "QW + 1 ml" refer to the emission from free and localized QW excitons, respectively. (b) QW PL peak energy vs T for samples N1 to N4 (squares, triangles, diamonds, and stars, respectively). Lines are the result of Varshni fits to the higher-T dependence of the QW emission energy for samples N2 to N4, yielding the localization energy of excitons in these QWs.

For sample N1, which has the same QW width as sample N2 but a higher barrier Al content (12% for sample N1 versus 6% for sample N2), the emission at 10 K is centered at 3.585 eV with $\delta = 15$ meV. Due to its larger barrier Al content, we expect deeper exciton localization for sample N1 than for sample N2. This deeper localization is evidenced by a larger exciton localization energy (Fig. 2 and Table I), as well as by a longer QW PL lifetime at 10 K, for the reasons mentioned above (Fig. 3). Note, however, that when extracting a localization energy from the T-dependence of the sample N1 emission energy, we had to use, when performing the Varshni fit,[24] a set of parameters that is different than that used for $Al_{0.06}Ga_{0.94}N$/GaN QWs. This is justified by the fact that the dilatation coefficients of $Al_{0.06}Ga_{0.94}N$ and $Al_{0.12}Ga_{0.88}N$ are not the same, yielding differences in the variation of the QW strain state for sample N1 and for samples N2, N3, and N4.

B. Time-resolved photoluminescence with temperature

We show in Fig. 4(a) the temperature dependence of the effective lifetime of QW excitons (τ) for samples N1 to N4.

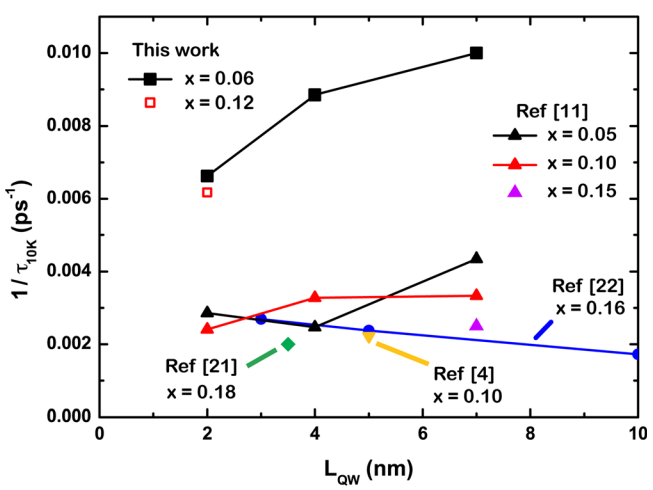

FIG. 3. (Color online) Experimental decay rates $1/\tau_{10K}$ at 10 K for excitons localized along nonpolar $Al_xGa_{1-x}N$/GaN QWs with respect to the QW width. Solid lines are guides for the eye. Squares: this work, a-plane $Al_{0.06}Ga_{0.94}N$/GaN and $Al_{0.12}Ga_{0.88}N$/GaN QWs (full and open squares, respectively) grown on bulk GaN. Triangles and circles: a-plane $Al_xGa_{1-x}N$/GaN QWs grown on ELO-GaN (Refs. 11 and 20). Diamonds: a-plane $Al_{0.18}Ga_{0.82}N$/GaN grown on sapphire (Ref. 19). Inverted triangles: m-plane $Al_{0.1}Ga_{0.9}N$/GaN QWs grown on γ-$LiAlO_2$ (Ref. 4).

In the low-temperature range (typically $T < 150$ K), we observe for all samples that increasing T leads to an increase of τ. As shown in Ref. 7, such behavior is direct evidence that exciton recombination in the temperature range of increasing τ is purely radiative. Therefore, in this temperature range, τ is nothing but the radiative decay time for excitons confined in the QWs. We note also that the measured radiative lifetime of a QW is determined, over the whole range of temperature, by the thermally activated exchanges between localized and delocalized QW states.[21,25]

In contrast, in the high-temperature range, we observe for all $Al_{0.06}Ga_{0.94}N$/GaN QW samples that τ decreases with temperature, indicating the activation of nonradiative recombination channels. We therefore need to understand, as nonradiative processes come into play at high T, what the dominant process that limits/promotes these nonradiative recombinations is. We can explore that in detail for the first time because in previous studies fast and efficient nonradiative carrier capture by dislocations washed out all the effects and limited the lifetimes, including at the lowest T.[5,6] As shown in Fig. 4(a) for $Al_{0.06}Ga_{0.94}N$/GaN structures, QW PL lifetimes do not steadily increase up to 300 K; rather, they start decreasing above some critical T and then tend toward a value of 100 to 250 ps at room temperature. Time- and temperature-resolved PL studies performed on high-quality III-arsenide QWs also revealed drops in both intensity and lifetime with increasing temperature. Such decreases were first ascribed to the thermal escape of charge carriers out of the QWs into barrier states, but with discrepancies of the associated activation energies reported by different groups. These energies indeed ranged from the electron-hole confinement energy[26] to half the total confinement energy,[27] or to the binding energy of the less confined species.[28,29] Gurioli *et al.* inferred that the discrepancies between the different reports simply came from the different methods used to extract the activation energies.[28] Based on their analysis of the temperature dependence of the QW PL effective lifetime, they deduced that the main nonradiative mechanism for QW charge carriers was related to the unipolar escape of carriers out of the QWs. In their model, Gurioli *et al.* simply modeled (Al,Ga)As barriers as nonradiative "sinks" for carriers. This model is not appropriate here considering the room-temperature PL spectrum shown in Fig. 2(a), in which intense PL from the (Al,Ga)N barriers is observed. Based on excitation dependent measurements, Weber *et al.*[30] then proposed competition between nonradiative recombinations at QW interface states[31,32] and the bipolar escape of carriers toward the barriers, followed by subsequent surface recombination, as the origin of the deviation between the different reports.

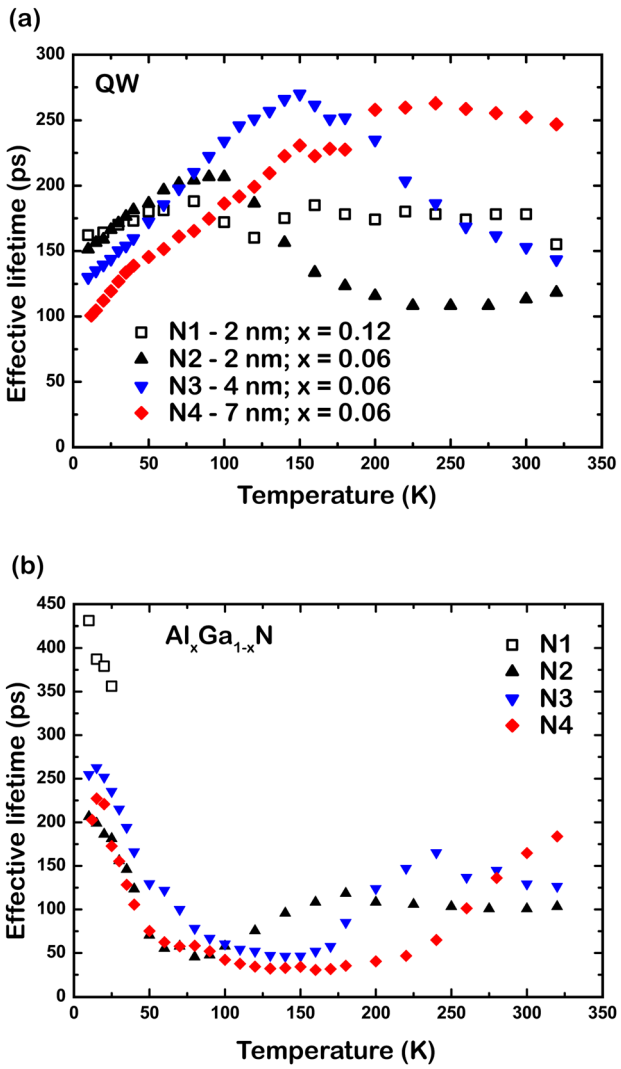

FIG. 4. (Color online) QW (a) and $Al_xGa_{1-x}N$ barrier (b) effective PL lifetimes as a function of T for samples N1 (black squares), N2 (black triangles), N3 (blue inverted triangles), and N4 (red diamonds). (a) The increase of QW PL lifetime with T is due to the combined delocalization of excitons in real and reciprocal spaces and is evidence of the negligible role played by nonradiative centers in the overall recombination mechanisms. (b) After a slight increase in lifetime between 10 K and 30 K due to deeper localization in the disordered alloy, the capture of $Al_xGa_{1-x}N$ excitons by the QWs results in a drastic reduction of the PL lifetime. At higher T, QW and barrier excitons get thermalized, resulting in an increase of the PL effective lifetime in the barriers.

Here, such a reduction in QW exciton lifetime cannot be ascribed to the capture of charge carriers by nonradiative states located in the QW or at its interfaces. First, the threading dislocation density and QW exciton room temperature diffusion length have been estimated, for the present samples, to be on the order of 2×10^5 cm^{-2} and 100 nm, respectively.[7] Therefore, only a small fraction of photogenerated excitons are affected by the presence of dislocations. Second, if mechanisms requiring the in-plane diffusion of QW excitons toward nonradiative point defects in the QW plane were involved in the drop of the QW PL lifetime at high-T, one would expect this process to be activated more easily for samples with shallower exciton localization. We observe experimentally the opposite behavior [Fig. 4(a)]: in sample N2, in which $E_{loc} = 14$ meV, the QW PL lifetime starts decreasing at $T = 100$ K, whereas this reduction starts at 150 and 240 K for samples N3 and N4, respectively.

Monitoring the (Al,Ga)N barrier PL lifetime in the whole 10-320 K temperature range allows one to further understand the dynamics of excitons at high T. First, the (Al,Ga)N PL lifetime decreases between 10 and 50 K. When T is increased within this range, excitons in the disordered alloy get spatially delocalized, and their decay is then dominated by capture into the QWs, assisted by LO phonon or

impurity scattering.[33] However, we observe an increase of the (Al,Ga)N PL lifetime in the highest-T range [Fig. 4(b)]. At 300 K, the emission from the barriers and from the QWs presents almost the same PL decay for all $Al_{0.06}Ga_{0.94}N$/GaN heterostructures, evidence of the full thermalization of exciton populations in the well and the barriers. We would like to bear in mind that in contrast to (Al,Ga)As/GaAs QWs,[26] no cladding layers are needed here for the observation at 300 K of both intense PL and non-instantaneous decay for those (Al,Ga)N barriers. In agreement with PL experiments on GaN surface QWs (Ref. 34) and on GaN nanocolumns a few tens of nanometers in diameter,[35] surface recombination is not efficient in low Al-content (Al,Ga)N, indicating that states induced by dangling bonds are energetically far from midgap in that material system.[36] In addition, we observe that passivating the surface of the present samples with SiN does not bring any significant change in terms of emission intensity or decay time at room temperature (not shown). It is nonetheless clear that charge carriers in the QWs and in the barriers are thermalized, and that the recombination lifetime of carriers in the disordered (Al,Ga)N barriers, whatever its radiative or nonradiative origin, is the limiting decay time for the whole charge carrier population in the heterostructure at 300 K.

C. Temperature dependence of quantum well and (Al,Ga)N barrier emission intensities

By analyzing the high-energy side of the PL emission peaks for QWs and barriers, we can determine the effective carrier temperature as a function of the lattice temperature (Fig. 5). We can therefore establish the temperature T_{th} above which exciton populations in the QWs and the barriers are fully thermalized. As expected for the thermal emission of carriers from a QW, the deeper the confinement, the higher the T_{th} (Table II). As relaxation processes are much faster than recombination mechanisms, QW PL and barrier PL show the same recombination dynamics for $T > T_{th}$ (Fig. 4). Still, we do not have, so far, any quantitative information—in terms of the activation energy—about the thermal escape of charge carriers out of the QWs. For that reason, we study in the following the evolution with T of the QW and (Al,Ga)N emission relative intensities. We denote as I_X^{QW} and I_X^{AlGaN} the emission intensities from the QWs and the (Al,Ga)N barriers, respectively. We consider I_X^{QW} as the sum of the emission intensities from free and localized QW excitons (I_{Xfr}^{QW} and I_{Xloc}^{QW}, respectively). Under thermodynamic equilibrium, the ratio between I_X^{AlGaN} and I_X^{QW} is given as

$$\frac{I_X^{AlGaN}}{I_X^{QW}} = \frac{I_X^{AlGaN}}{I_{Xfr}^{QW} + I_{Xloc}^{QW}} \propto \frac{N_X^{AlGaN}/\tau_r^{AlGaN}}{N_{Xfr}^{QW}/\tau_{r,Xfr}^{QW} + N_{Xloc}^{QW}/\tau_{r,Xloc}^{QW}}. \quad (1)$$

N_{Xfr}^{QW} and N_{Xloc}^{QW} are, respectively, the free and localized QW exciton densities, which decay radiatively within the characteristic times $\tau_{r,Xloc}^{QW}$ and $\tau_{r,Xfr}^{QW}$, and N_X^{AlGaN} represents the density of excitons in (Al,Ga)N, with a radiative lifetime τ_r^{AlGaN}. The intensity ratio between the emissions from the QWs and the (Al,Ga)N barriers is plotted as a function of the inverse of T in Fig. 6 for samples N2, N3, and N4. Note that we are not able to plot this ratio for sample N1 because the emission from the $Al_{0.12}Ga_{0.88}N$ barriers is too weak for $T > 50$ K. As expected, the deeper the confinement, the smaller the emission intensity ratio between the barriers and the QWs (Fig. 6). Still, the T-dependence of I_X^{AlGaN}/I_X^{QW} is not monoexponential, indicating that the thermal escape of charge carriers from the QW to the (Al,Ga)N barriers cannot be simply described with an activation energy. This arises first from the fact that the evolutions with temperature of QW and (Al,Ga)N barrier radiative lifetimes are not the same: whereas the former increases with T,[21,25,37] the temperature-dependence of the latter is not straightforward, as one deals with excitons in a disordered three-dimensional alloy. In addition, one has to account for the fact that due to their

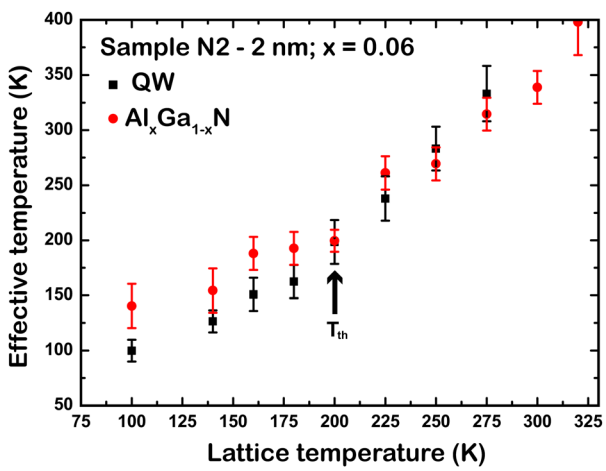

FIG. 5. (Color online) Effective QW (squares) and barrier (circles) carrier temperature with respect to the lattice temperature for sample N2, obtained from the analysis of QW and $Al_xGa_{1-x}N$ high-energy side of PL spectra. Above 200 K, QW and $Al_xGa_{1-x}N$ carriers effective temperatures are identical, evidencing full thermalization of both exciton populations. The arrow points the temperature T_{th} above which $Al_xGa_{1-x}N$ barriers and QW carrier populations are fully thermalized.

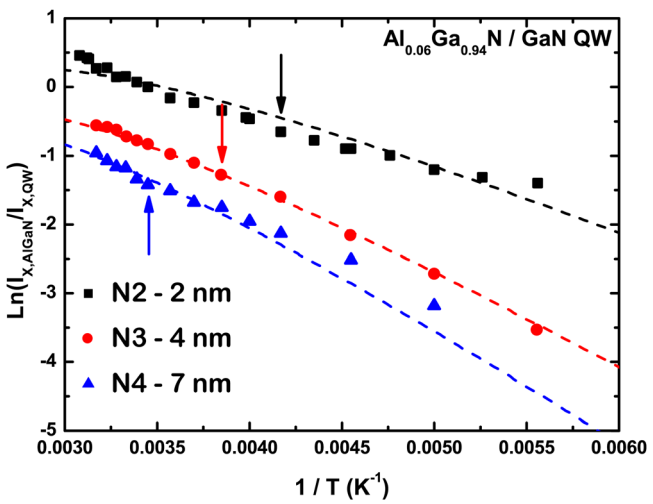

FIG. 6. (Color online) Experimental time-integrated intensity ratio between barrier and QW emissions plotted against (1/T) for samples N2, N3 and N4 (squares, circles and triangles). Arrows shows the temperature T_{th} above which full thermalization is achieved between QW and $Al_xGa_{1-x}N$ barriers. Dashed lines are the calculated ratio between $Al_xGa_{1-x}N$ and QW emission intensities versus the inverse of temperature using Eq. (10) and the parameters gathered in Table II.

TABLE II. QW localization energy E_{loc} calculated when accounting for a one-monolayer fluctuation of the QW width. Calculated QW and barrier exciton binding energies ($E_{B,QW}$ and $E_{B,AlGaN}$, respectively), energy differences ΔE_e (ΔE_h) between barrier conduction (valence) band and ground-state energy of the QW, and total electron-hole confinement energies ΔE_{th}. The temperatures T_{th} above which barrier and QW excitons are thermalized are obtained from the procedure shown in Figure 5.

Samples	Calculations						Experiments
No.	E_{loc}(meV)	ΔE_e(meV)	ΔE_h(meV)	E_b^{QW} (meV)	E_b^{AlGaN}(meV)	ΔE_{th}(meV)	T_{th}(K)
N1	14	122	78	48	29	219	–
N2	8	43	33	42	27	91	200
N3	3	74	42	40	27	129	260
N4	1	97	47	35	27	152	290

respective two- and three-dimensionalities, the QWs and the (Al,Ga)N barriers do not present the same density of states. In the following, we consequently measure QW and (Al,Ga)N barrier radiative lifetimes as a function of T (Sec. III.D). We then compute, in Sec. III.E, the respective densities of excitons, electrons, and holes in both the two-dimensional QWs and the three-dimensional (Al,Ga)N barriers, with respect to T. Finally, we compare the measured T-dependence of I_X^{AlGaN}/I_X^{QW} with the computed one.

D. GaN quantum well and (Al,Ga)N barrier radiative lifetimes with temperature

As shown in Eq. (1), it is first mandatory to know the T-dependence of both QW and barrier radiative lifetimes in order to correctly fit the evolution of $\ln(I_X^{AlGaN}/I_X^{QW})$ with T. Concerning the radiative lifetime of QW excitons, we apply the method described in our previous study.[7] As stated above, we observe for all QW samples purely radiative exciton recombinations in the low-T range. The radiative lifetime for QW excitons over the whole 10-320 K temperature range is thus simply obtained via linear extrapolation to high temperatures of the increase in QW effective decay time observed in Fig. 4(a) at low temperatures.[21,25]

In order to obtain the temperature dependence of the exciton radiative lifetime in the $Al_{0.06}Ga_{0.94}N$ barriers, we performed time-resolved PL experiments on a 190 nm thick $Al_{0.06}Ga_{0.94}N$ layer (sample N5). Because the total thickness of the QW barriers for samples N2 to N4 is also equal to 190 nm, the density of states for excitons in the (Al,Ga)N barriers of samples N2, N3, and N4 is the same as that in sample N5, and their radiative lifetimes are therefore comparable. We plot in Fig. 7 the effective PL decay time for sample N5 with respect to T. At 10 K, the sample N5 emission decays within a characteristic lifetime of 204 ps. Increasing T up to 100 K leads to a reduction of the decay time to 25 ps. This lifetime then stays nearly constant for higher T. In parallel, over the whole temperature range, increasing temperature leads to a decrease of the initial PL intensity of sample N5. Assuming that the decay is purely radiative at 10 K (which is reasonable, as at such a low temperature most of the excitons are localized on potential fluctuations), we can extract the $Al_{0.06}Ga_{0.94}N$ radiative lifetime with respect to the temperature (Fig. 7). We find that it does increase nearly exponentially with temperature, reaching ~5 ns at 300 K. We tentatively attribute this exponential dependence of the (Al,Ga)N radiative lifetime with respect to T to the thermal exchange between excitons and free carriers, as modeled and observed experimentally in Ref. 38. As a consequence, and contrary to what is observed for excitons confined in GaN QWs, the decay of carriers in (Al,Ga)N is mainly nonradiative for $T > 100$ K. As GaN QWs and (Al,Ga)N barriers exhibit similar threading dislocation densities, we infer that such a difference between the nonradiative recombination rates in GaN and (Al,Ga)N might arise from a higher cation vacancy density in the disordered alloy, because for the present samples, the GaN QWs and the (Al,Ga)N barriers were grown at the same temperature.

E. Fitting procedure for the thermal escape of charge carriers from the quantum well to the barriers

Now, we need to estimate, for all T, the respective densities of excitons in the QWs and in the barriers. This can be done numerically with a model that accounts for the following:

(i) the thermally activated delocalization of excitons along the QW plane,
(ii) the dissociation of excitons into free carriers in both the QWs and the (Al,Ga)N barriers, and

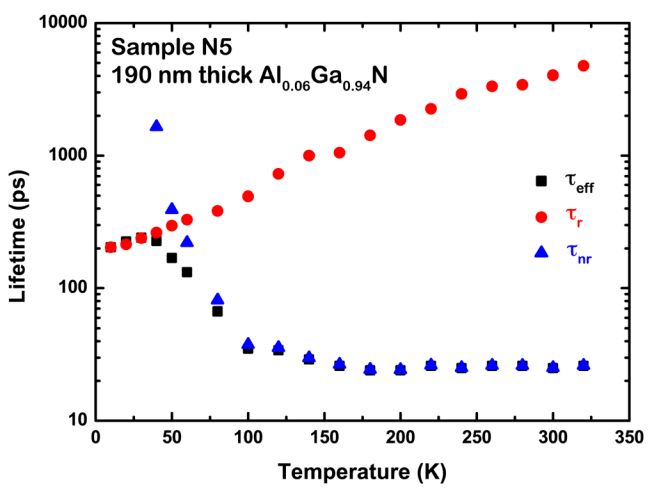

FIG. 7. (Color online) Temperature-dependence of effective (τ_{eff}), radiative (τ_r) and nonradiative (τ_{nr}) decay times (squares, circles and triangles, resp.) for a 190 nm thick $Al_{0.06}Ga_{0.94}N$ layer (sample N5).

(iii) the thermal escape of free electrons and holes from the two-dimensional QWs to the three-dimensional barriers.

First, the thermal equilibrium between localized and free excitons in the quantum well is given by the following equation:

$$\frac{N_{Xloc}^{QW}}{N_{Xfr}^{QW}} = \frac{N_D \pi \hbar^2}{2MkT} exp\left[\frac{E_{loc}}{kT}\right]. \quad (2)$$

N_{Xloc}^{QW} and N_{Xfr}^{QW} denote the localized and free QW exciton densities, respectively, and N_D, E_{loc}, and M are the density of localization states, the exciton localization energy, and the exciton mass, respectively. Similar to our previous work,[7] we take $M = 1.2m_0$ and $N_D = 3 \times 10^{12}\,\mathrm{cm}^{-2}$, and E_{loc} is estimated via envelope calculations (Table II). With N_e and N_h electron and hole densities, the mass action law between free carriers and free excitons in the two-dimensional QW is[39,40]

$$\frac{N_e^{QW} N_h^{QW}}{N_X^{QW}} = \frac{\mu kT}{2\pi\hbar^2} exp\left[-\frac{E_b^{QW}}{kT}\right], \quad (3)$$

whereas in the three-dimensional barriers it is

$$\frac{N_e^{AlGaN} N_h^{AlGaN}}{N_X^{AlGaN}} = L\left(\frac{\mu kT}{2\pi\hbar^2}\right)^{3/2} exp\left[-\frac{E_b^{AlGaN}}{kT}\right]. \quad (4)$$

E_b^{QW} and E_b^{AlGaN} are the exciton binding energies in the QWs and in (Al,Ga)N, respectively, and μ is the exciton reduced mass. We have calculated E_b^{QW} through envelope function calculations for the whole set of samples (Table II). Note that in our calculations, we have separated the in-plane and on-axis relative motions of the electron and hole. We therefore slightly underestimate the binding energy for QWs N3 and N4, which are wider than 1.4 times the exciton Bohr radius in bulk GaN.[41] We also consider the electron and hole effective masses to be the same in the QWs and in the low Al-content ternary alloy. However, we take E_b^{AlGaN} as equal to 27 and 29 meV in $Al_{0.06}Ga_{0.94}N$ and $Al_{0.12}Ga_{0.88}N$, respectively.[42] Finally, $L = 190\,\mathrm{nm}$ is the total thickness of the (Al,Ga)N barriers. Under the assumption that electron and hole populations follow a Boltzmann distribution, and accounting only for the first QW confined state, the ratio of the QW electron density N_e^{QW} (hole density N_h^{QW}) to that in the barrier N_e^{AlGaN} (N_h^{AlGaN}) is given in Eq. (5) [Eq. (6)].

$$\frac{N_e^{AlGaN}}{N_e^{QW}} = \frac{\tilde{N}_e^{AlGaN} L}{\tilde{N}_e^{QW}} \exp\left[-\frac{\Delta E_e}{kT}\right] \quad (5)$$

$$\frac{N_h^{AlGaN}}{N_h^{QW}} = \frac{\tilde{N}_h^{AlGaN} L}{\tilde{N}_h^{QW}} \exp\left[-\frac{\Delta E_h}{kT}\right] \quad (6)$$

ΔE_e (ΔE_h) is the energy difference between barrier conduction (valence) band and the electron (hole) ground-state of the QW. As was the case for QW exciton binding energies, ΔE_e and ΔE_h can be obtained via finite difference calculations (Table II). $\tilde{N}_e^{AlGaN}$ and $\tilde{N}_h^{AlGaN}$ are the three-dimensional effective electron and hole densities of states for the barriers, and $\tilde{N}_e^{QW}$ and $\tilde{N}_h^{QW}$ are the QW two-dimensional effective electron and hole densities of states. Considering that the electric charge is conserved and that the material is electrically neutral, one gets

$$N_e^{AlGaN} + N_e^{QW} + N_X^{AlGaN} + N_{Xfr}^{QW} + N_{Xloc}^{QW} = N_{tot}, \quad (7)$$

$$N_h^{AlGaN} + N_h^{QW} + N_X^{AlGaN} + N_{Xfr}^{QW} + N_{Xloc}^{QW} = N_{tot}. \quad (8)$$

The system made of Eqs. (2) to (8) is then solved to obtain the T-dependence of each charge carrier density for the whole set of samples. It is worth emphasizing that we do not have to account explicitly for the escape of excitons from the GaN QWs toward the (Al,Ga)N barriers. In other words, at thermal equilibrium, the dissociation of QW excitons into free electron hole pairs has to be activated before there can be excitons in the (Al,Ga)N barriers. The result of our calculations, displayed in Fig. 8, reproduces what we observe for the respective QW and (Al,Ga)N emission intensities for samples N1 to N4. In agreement with the intense PL seen at room temperature for the $Al_{0.06}Ga_{0.94}N$ barriers of sample N2 [Fig. 2(a)], we compute for this sample (Al,Ga)N and QW exciton densities of the same order of magnitude at 320 K. In contrast, for sample N1, we compute an exciton density in the barriers that is two orders of magnitude smaller than the QW exciton density, explaining why even at 320 K we do not detect any PL from the $Al_{0.12}Ga_{0.88}N$ barriers. More quantitatively, in the case in which $N_{Xloc}^{QW} \ll N_{Xfr}^{QW}$ (i.e., for samples N2, N3, and N4 when $T > 150\,\mathrm{K}$), it is also possible to express analytically the ratio of the (Al,Ga)N exciton density to that of the QWs.

$$\ln\left(\frac{N_X^{AlGaN}}{N_{Xfr}^{QW}}\right) = \frac{1}{2}\ln\left(\frac{m_e m_h}{\mu}\frac{kTL^2}{32\pi\hbar^2}\right) - \frac{\Delta E_e + \Delta E_h + E_b^{QW} - E_b^{AlGaN}}{kT}. \quad (9)$$

The first term on the right-hand side of Eq. (9) is a geometrical term that accounts for the difference in the density of states between the barriers and the QWs. The numerator of the second term on the right-hand side of Eq. (8) is equivalent to an activation energy for the escape of excitons from the QWs toward the (Al,Ga)N barriers. However, this activation energy ΔE_{th} depends not only on the total confinement energy $\Delta E_e + \Delta E_h$ but also on the difference between QW and (Al,Ga)N barrier exciton binding energies. When the (Al,Ga)N barrier and QW populations are in thermal equilibrium, the ratio between the (Al,Ga)N and QW exciton densities does not depend on the total carrier density in the structure. By inserting Eq. (9) into Eq. (1), we get the intensity ratio between (Al,Ga)N and QW time-integrated PL,

$$\ln\left(\frac{I_X^{AlGaN}}{I_{Xfr}^{QW}}\right) = A + \ln\left(\frac{\tau_{r,Xfr}^{QW}}{\tau_{r,X}^{AlGaN}}\right) + \frac{1}{2}\ln\left(\frac{m_e m_h}{\mu}\frac{kTL^2}{32\pi\hbar^2}\right) - \frac{\Delta E_e + \Delta E_h + E_b^{QW} - E_b^{AlGaN}}{kT}, \quad (10)$$

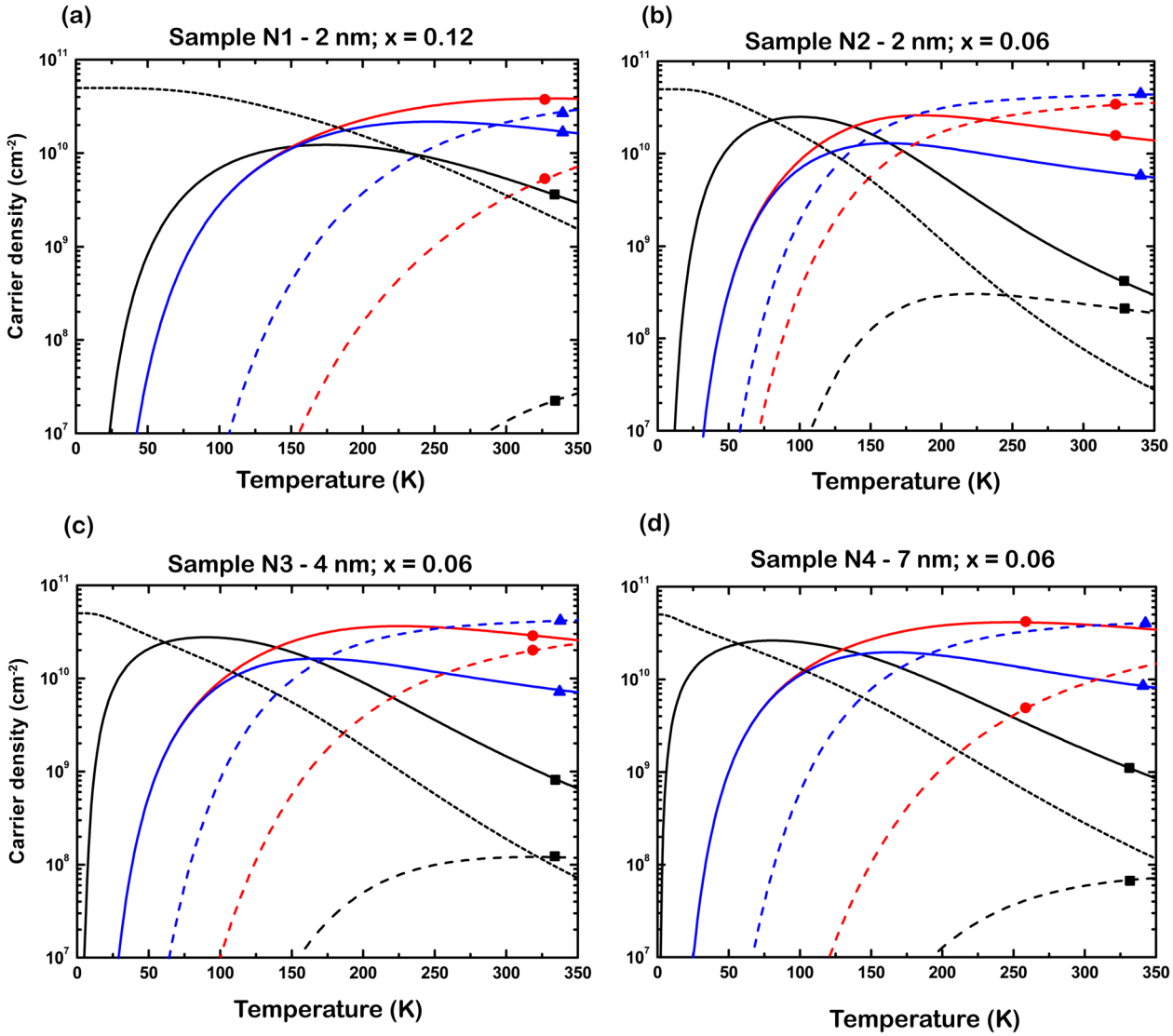

FIG. 8. (Color online) Calculated free exciton, electron and hole densities (black squares, red circles and blue triangles, resp.) in the QW (solid lines) and in the $Al_xGa_{1-x}N$ barriers (dashed lines) using the parameters gathered in Table II, for a photogenerated pair density of 5×10^{10} cm^{-2}. Black dotted lines show the density of localized QW excitons. Panels (a), (b), (c) and (d) correspond respectively to samples N1, N2, N3 and N4.

with A being a constant. We show in Fig. 6 the best fits to the intensity ratio between QW and (Al,Ga)N barrier emissions as a function of the inverse of T. Despite the simplicity of our model, the computed T-dependence of the ratio between (Al,Ga)N and QW emission intensities reproduces the trends observed experimentally for $\ln(I_X^{AlGaN}/I_{Xfr}^{QW})$. We underline the fact that the geometrical term in Eq. (10) has a negligible influence on the evolution of $\ln(I_X^{AlGaN}/I_{Xfr}^{QW})$ with T. By extension, the fact that our model accounts for exciton A excited states as well as for B and C exciton branches should not significantly modify the result of our calculations, as this would change the absolute value but not the T-dependence of the geometrical term in Eq. (10). Conversely, uncertainties regarding the actual QW width and the barrier Al content, as well as the conduction-band offset ratio, are more likely to introduce discrepancies between experimental and calculated emission intensity ratios. In any case, we reproduce for all $Al_{0.06}Ga_{0.94}N$/GaN QW samples the relative increase of I_X^{AlGaN}/I_{Xfr}^{QW} in the high-T range.

From our detailed study, three points should be emphasized. First, we have shown that thanks to the use of GaN substrates grown via a combination of the high-pressure solution method and HVPE, we were able to fabricate (Al,Ga)N/GaN QWs in which recombinations are dominated by radiative phenomena over a large temperature range (up to 240 K for sample N4). In contrast to what occurs in (In,Ga)N/GaN QWs,[43] our observation was made in QWs with low localization energy. It is consequently possible to achieve nonpolar room-temperature UV emitters combining a rather narrow emission line with good radiative efficiency at 300 K. Second, we have demonstrated that the mechanism limiting the efficiency of the QWs was due to the thermal escape of free charge carriers toward barriers and their subsequent nonradiative recombination. Thanks to the elimination of built-in electric fields in a-plane heterostructures, we thus propose to tackle the thermal escape of carriers through the growth of thick QWs rather than through an increase in the barrier Al-content, which is important from the defect/

strain generation point of view. For instance, we determined via envelope function calculations that an *a*-plane (Al,Ga)N/GaN QW with a thickness of 7 nm and a barrier Al content of 8% exhibits a ΔE_e and ΔE_h of 133 and 61 meV, respectively. For such a structure, one should observe nearly purely radiative recombination at 300 K, as we estimate from Eq. (9) that it presents $N_X^{AlGaN} < 0.01\ N_X^{QW}$ at room temperature. Finally, our model shows that there is no such thing as a direct escape of excitons out of a QW to the barriers, and that when describing the temperature-dependence of the relative QW and barrier exciton densities by using an activation energy, one has to account for the total confinement energy and for the difference between the QW and (Al,Ga)N barrier exciton binding energies. A thorough study of the mechanisms limiting charge carrier lifetime in (Al,Ga)N barriers should allow for further improvement of the efficiency of UV-light emitters based on so-proposed nonpolar (Al,Ga)N/GaN QWs with a low Al content barrier.

IV. CONCLUSION

In conclusion, we have grown on the *a*-facet of bulk GaN crystals (Al,Ga)N/GaN QWs of various widths and barrier Al contents. The absence of stacking faults and the low dislocation density of these structures allow for the direct monitoring via time-resolved photoluminescence of the increase of the QW radiative lifetime with temperature. In the high temperature range, a drop in the QW photoluminescence lifetime is always accompanied by an increase in the barrier emission lifetime, until both emissions follow the same dynamics. Supported by a model accounting for the thermodynamic equilibrium between excitons and free carriers in the QWs and the (Al,Ga)N barriers, we demonstrate that at high temperatures, the nonradiative recombination of charge carriers in the (Al,Ga)N barriers is the mechanism limiting the photoluminescence lifetime of excitons confined in the QWs.

ACKNOWLEDGMENTS

We acknowledge financial support from the Swiss National Science Foundation through Project No. 129715 and from the Polish Ministry of Science and Higher Education (Project Nos. NN202 010134 and NN202 131339). The work was partially supported by the European Union within European Regional Development Fund through Innovative Economy Grant No. POIG.01.01.02-00-008/08. We also thank R. Rochat, N. Leiser, Y. Trolliet, and D. Trolliet for their technical assistance.

[1]F. Bernardini and V. Fiorentini, Phys. Rev. B **57**, R9427 (1998).
[2]R. Langer, J. Simon, V. Ortiz, N. T. Pelekanos, A. Barski, R. André, and M. Godlewski, Appl. Phys. Lett. **74**, 3827 (1999).
[3]N. F. Gardner, G. O. Müller, Y. C. Shen, G. Chen, S. Watanabe, W. Götz, and M. R. Krames, Appl. Phys. Lett. **91**, 243506 (2007).
[4]P. Waltereit, O. Brandt, A. Trampert, H. T. Grahn, J. Menniger, M. Ramsteiner, M. Reiche, and K. H. Ploog, Nature **406**, 865 (2000).
[5]T. J. Badcock, P. Dawson, M. J. Kappers, C. McAleese, J. L. Hollander, C. F. Johnston, D. V. Sridhara Rao, A. M. Sanchez, and C. J. Humphreys, Appl. Phys. Lett. **93**, 101901 (2008).
[6]P. Corfdir, P. Lefebvre, L. Balet, S. Sonderegger, A. Dussaigne, T. Zhu, D. Martin, J.-D. Ganière, N. Grandjean, and B. Deveaud-Plédran, J. Appl. Phys. **107**, 043524 (2010).
[7]P. Corfdir, J. Levrat, A. Dussaigne, P. Lefebvre, H. Teisseyre, I. Grzegory, T. Suski, J.-D. Ganière, N. Grandjean, and B. Deveaud-Plédran, Phys. Rev. B **83**, 245326 (2011).
[8]B. Lucznik, B. Pastuszka, G. Kamler, I. Grzegory, and S. Porowski, "Growth of bulk GaN crystals by HVPE on single crystalline GaN seeds," in *Technology of Gallium Nitride Crystal Growth*, edited by D. Ehrentraut, E. Meissner, and M. Boćkowski (Springer-Verlag, Heidelberg, 2010), pp. 61–78.
[9]A. Bellabchara, P. Lefebvre, P. Christol, and H. Mathieu, Phys. Rev. B **50**, 11840 (1994).
[10]D. Bimberg, J. Christen, T. Fukunaga, H. Nakashima, D. E. Mars, and J. N. Miller, J. Vac. Sci. Technol. B **5**, 1191 (1987).
[11]A. Dussaigne, P. Corfdir, J. Levrat, T. Zhu, D. Martin, P. Lefebvre, J.-D. Ganière, R. Butté, B. Deveaud-Plédran, N. Grandjean, Y. Arroyo, and P. Stadelmann, Semicond. Sci. Technol. **26**, 025012 (2011).
[12]E. Feltin, D. Simeonov, J.-F. Carlin, R. Butté, and N. Grandjean, Appl. Phys. Lett. **90**, 021905 (2007).
[13]K. Kornitzer, T. Ebner, K. Thonke, R. Sauer, C. Kirchner, V. Schwegler, M. Kamp, M. Leszczynski, I. Grzegory, and S. Porowski, Phys. Rev. B **60**, 1471 (1999).
[14]G. Salviatti, M. Albrecht, C. Zanotti-Fregonara, N. Armani, M. Mayer, Y. Shreter, M. Guzzi, Y. V. Melnik, K. Vassilevski, V. A. Dmitiev, and H. P. Strunk, Phys. Status Solidi. A **171**, 325 (1999).
[15]R. Liu, A. Bell, F. A. Ponce, C. Q. Chen, J. W. Yang, and M. A. Khan, Appl. Phys. Lett. **86**, 021908 (2005).
[16]P. Corfdir, J. Ristić, P. Lefebvre, T. Zhu, D. Martin, A. Dussaigne, J. D. Ganière, N. Grandjean, and B. Deveaud-Plédran, Appl. Phys. Lett. **94**, 201115 (2009).
[17]B. Deveaud, J. Y. Emery, A. Chomette, B. Lambert, and M. Baudet, Appl. Phys. Lett. **45**, 1078 (1984).
[18]M. Leroux, N. Grandjean, M. Laügt, J. Massies, B. Gil, P. Lefebvre, and P. Bigenwald, Phys. Rev. B **58**, R13371 (1998).
[19]T. J. Badcock, S. Hammersley, M. J. Kappers, C. J. Humphreys, and P. Dawson, Phys. Status Solidi C **7**, 1894 (2010).
[20]G. A. Garrett, H. Shen, M. Wraback, B. Ilmer, B. Haskell, J. S. Speck, S. Keller, S. Nakamura, and S. P. DenBaars, Phys. Status Solidi A **202**, 846 (2005).
[21]D. S. Citrin, Phys. Rev. B **47**, 3832 (1993).
[22]E. T. Rashba and G. E. Gurgenishvili, Fiz. Tverd. Tela (Leningrad) **4**, 759 (1962) [Sov. Phys. Solid State **4**, 759 (1962)].
[23]J. Bellessa, V. Voliotis, R. Grousson, X. L. Wang, M. Ogura, and H. Matsuhata, Phys. Rev. B **58**, 9933 (1998).
[24]Y. P. Varshni, Physica **34**, 149 (1967).
[25]M. Colocci, M. Gurioli, and J. Martinez-Pastor, J. Phys. IV **3**, C5–3 (1993).
[26]G. Bacher, C. Hartmann, H. Schweizer, T. Held, G. Mahler, and H. Nickel, Phys. Rev. B **47**, 9545 (1993).
[27]P. Michler, A. Hangleiter, M. Moser, M. Geiger, and F. Scholz, Phys. Rev. B **46**, 7280 (1992).
[28]M. Gurioli, J. Martinez-Pastor, M. Colocci, C. Deparis, B. Chastaingt, and J. Massies, Phys. Rev. B **46**, 6922 (1992).
[29]M. Vening, D. J. Dunstan, and K. P. Homewood, Phys. Rev. B **48**, 2412 (1993).
[30]S. Weber, W. Limmer, K. Thonke, R. Sauer, K. Panzlaff, G. Bacher, H. P. Meier, and P. Roentgen, Phys. Rev. B **52**, 14739 (1995).
[31]M. Krahl, D. Bimberg, R. K. Bauer, D. E. Mars, and J. N. Miller, J. Appl. Phys. **67**, 434 (1990).
[32]H. Hillmer, A. Forchel, R. Sauer, and C. W. Tu, Phys. Rev. B **42**, 3220 (1990).
[33]B. Deveaud, A. Chomette, D. Morris, and A. Regreny, Solid State Commun. **83**, 367 (1993).
[34]J. F. Muth, X. Zhang, A. Cai, D. Fothergill, J. C. Roberts, P. Rajagopal, J. W. Cook, Jr., E. L. Piner, and K. J. Linthicum, Appl. Phys. Lett. **87**, 192117 (2005).
[35]P. Corfdir, P. Lefebvre, J. Ristić, P. Valvin, E. Calleja, A. Trampert, J.-D. Ganière, and B. Deveaud-Plédran, J. Appl. Phys. **105**, 013113 (2009).
[36]D. D. Nolte, Solid State Electron. **33**, 295 (1990).
[37]L. C. Andreani, F. Tassone, and F. Bassani, Solid State Commun. **77**, 641 (1991); model revised in L. C. Andreani, in *Confined Electrons and Photons: New Physics and Devices*, edited by E. Burstein and C. Weisbuch (Plenum, New York, 1994).
[38]A. Feltrin, J. L. Staehli, B. Deveaud, and V. Savona, Phys. Rev. B **69**, 233309 (2004).
[39]M. Colocci, M. Gurioli, and A. Vinattieri, J. Appl. Phys. **68**, 2809 (1990).

[40]D. S. Chemla, Helv. Phys. Acta **56**, 607 (1983).
[41]G. Bastard, E. E. Mendez, L. L. Chang, and L. Esaki, Phys. Rev. B **26**, 1974 (1982).
[42]We consider that the exciton binding energy in $Al_xGa_{1-x}N$ varies linearly with x. The exciton binding energy in AlN is 55 meV, as reported in M. Feneberg, R. A. R. Leute, B. Neuschl, K. Thonke, and M. Bickermann, Phys. Rev. B **82**, 075208 (2010).
[43]R. A. Oliver, S. E. Bennett, T. Zhu, D. J. Beesley, M. J. Kappers, D. W. Saxey, A. Cerezo, and C. J. Humphreys, J. Phys. D: Appl. Phys. **43**, 354003 (2010).